

Control of tethered airfoils for a new class of wind energy generator

M. Canale, L. Fagiano, M. Ippolito, M. Milanese

Abstract—The paper investigates the control of tethered airfoils in order to devise a new class of wind generators able to overcome the main limitations of the present aeolian technology based on wind mills. A model taken from the literature is used to simulate the dynamic of a kite which can be controlled by suitably pulling two lines. Energy is generated by a cycle composed of two phases, indicated as the traction and the recovery one. The control unit has two electric drives which act as motors in pulling the lines for controlling the flight or for recovering the kite and as generators if the kite pulls the lines. In each phase, control is obtained by “fast” implementations of suitable NMPC designs. In the traction phase the control is designed such that the kite pulls the lines, maximizing the amount of generated energy. When the maximal length of the lines is reached, the control enters the recovery phase and the kite is driven to a region where the lines can be pulled by the motors until the minimal length is reached, spending a small fraction of the energy generated in the traction phase, and a new traction phase is undertaken. Simulation results are presented, related to a small scale prototype whose construction is undergoing at our laboratory.

I. INTRODUCTION

Energy generation has become an urgent, strategic issue at the global scale. At present, about 80% of world electric energy is produced from thermal plants making use of fossil sources (oil, gas, coal). The economical, geopolitical and environmental problems related to such sources are becoming every day more and more evident. Nuclear plants have their own problems related to security aspects and radioactive waste management. For these reasons it is of primary importance for the scientific community to explore and support new renewable energy technologies, able to provide more efficient solutions than the existing ones to the severe energy shortage of the planet.

Wind turbines are currently the largest source of electric power produced with renewable energy (excluding hydro power plants) [1]. However, they require heavy towers, foundations and huge blades, which make a significant impact on the environment, require massive investments and long-term amortization periods. All these problems reflect in electric energy production costs that are not yet competitive, in strict economic sense, with the ones of thermal generators, despite recent large rises of oil and gas prices. Moreover, wind farms have wide problems of social acceptance due their territory

Supported by Regione Piemonte under the Project “Controllo di aquiloni di potenza per la generazione eolica di energia” and by Ministero dell’Università e della Ricerca of Italy, under the National Project “Robustness and optimization techniques for high performances control systems”.

M. Canale, L. Fagiano and M. Milanese are with Dip. di Automatica e Informatica, and Respira Lab, Politecnico di Torino, Italy. M. Ippolito is with Sequoia Automation and Respira Lab, Politecnico di Torino, Italy
Email: massimo.canale@polito.it, lorenzo.fagiano@polito.it, m.ippolito@sequoiaonline.com, mario.milanese@polito.it

occupation, which is unacceptably higher than for thermal plants of the same power (up to 200-300 times).

This paper illustrates a first study conducted at Respira Lab, a laboratory founded at Politecnico di Torino to design and build a new class of wind generator, indicated as KiteGen, aimed to overcome the above limitations. The key idea (patented by one of the authors, [2]) is to capture wind energy by means of tethered airfoils (e.g. power kites used for surfing or sailing, see Fig. 1), whose flight is suitably driven by an automatic control unit. It is expected that wind



Fig. 1. A kite surfer

generator of this type will have a territory occupation much lower than a wind farm of the same power (by a factor up to 50-100) and much lower electric energy production costs (by a factor up to 10-20). The reasons of such a dramatic potential improvements are that for both generators the energy captured from the wind approximately grows with the cube of wind speed and linearly with the wind intercepted front area. Assuming that the airfoils can fly up to several hundred meters of altitude, KiteGen can take advantage of the fact that as altitude on the ground increases, wind is stronger and more constant, see Fig. 2. For example, at 800 m the wind speed doubles with respect to 100 m (mean altitude at which the largest wind mill operate) and, being all other parameters constant, the generated power is eight times greater. Moreover, with lines several hundred meters long, the airfoils can intercept a wind front area much larger than the intercepted area of wind mills, which for structural limits cannot go beyond the size intercepted by 90 m rotor diameters of big 5 MW towers (at present suitable only for off-shore installations, see [3]).

As a first step, the KiteGen project will realize a small scale prototype (see Fig. 3) to show the capability of controlling the flight of a single kite, by pulling the two lines which hold it, in such a way to extract a significant amount of energy. In this paper we investigate such a capability in simulation,



Fig. 2. Variation in the wind speed, as a function of the altitude, based on the average European wind speed (3 m/s at ground level).



Fig. 3. KiteGen small scale prototype

employing the kite model used in [4]. The overall maneuver is composed of two phases: the traction and the recovery ones. The control unit (see Fig. 4) has two electric actuators which act as motors in pulling the lines for controlling the flight or for recovering the kite and as generators if the lines length increases when pulled by the kite. In the traction phase the control is designed such that the kite pulls the lines, so that a certain amount of energy is generated. When the maximal length of the lines is reached, the control enters into the recovery phase, where the kite is driven to a region where the lines can be pulled by the motors until the minimal length is reached, spending a small fraction of the energy generated in the traction phase and a new traction phase is undertaken. The control design is here carried on using a Fast implementation of a Predictive Controller (FMPC) as proposed in [5] and [6]. Indeed, the design is formulated as an optimization problem (power maximization in the traction phase and minimization in the recovery phase) with state and input constraints, since for example the kite height on the ground cannot be negative and lines pulling and its rate of variation cannot exceed given limits. From this point of view, Model Predictive Control (MPC) appears to be an appropriate technique. However, a “fast” implementation is

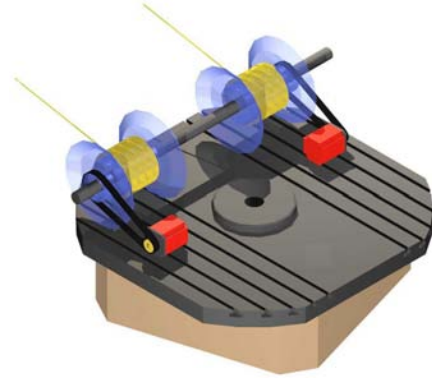


Fig. 4. KiteGen control unit

needed, in order to allow the real time control at the required sampling time (of the order of 0.1 s). It can be noted that MPC technique has been employed in [4] for kite control. However, in [4], the concern was not on energy generation, but the aim was to stabilize a given unstable periodic orbit that can be obtained for constant line length. In this paper, in order to investigate the energy extraction, the line length is not supposed to be constant and no kite trajectory is preassigned to be tracked. The derived kite trajectory is on the contrary determined by the optimization of the generated energy.

The paper is organized as follows. In Section II the used kite model is presented. In Section III the MPC setup is formulated and the control specifications are introduced; in Section IV the used technique for the fast control implementation is briefly described. The simulation results related to the small scale prototype whose construction is undergoing at Respira Lab are presented in Section V. Some conclusions and future developments are reported in Section VI.

II. KITE MODEL

The model originally developed in [4] is employed to describe the kite dynamics. A fixed cartesian coordinate system (X, Y, Z) is considered, with X axis aligned with the nominal wind speed vector direction. Wind speed vector is represented as $\vec{W}_t = \vec{W}_0 + \vec{W}_t$, where \vec{W}_0 is the nominal wind, supposed to be known and expressed in (X, Y, Z) as:

$$\vec{W}_0 = \begin{pmatrix} W_x(Z) \\ 0 \\ 0 \end{pmatrix} \quad (1)$$

$W_x(Z)$ is a known function which gives the wind nominal speed at a certain altitude Z . The term \vec{W}_t may have components in all directions and is not supposed to be known, accounting for wind unmeasured turbulence.

A spherical coordinate system is also considered, centered where the kite lines are constrained to the ground. In this system, the kite position is given by its distance r from the origin and by the two angles θ and ϕ , as depicted in Fig. 5, which also shows the three basis vectors e_θ , e_ϕ and e_r of a local coordinate system. These basis vectors are expressed

in the fixed cartesian system (X, Y, Z) by:

$$\begin{pmatrix} e_\theta & e_\phi & e_r \end{pmatrix} = \begin{pmatrix} \cos(\theta) \cos(\phi) & -\sin(\phi) & \sin(\theta) \cos(\phi) \\ \cos(\theta) \sin(\phi) & \cos(\phi) & \sin(\theta) \sin(\phi) \\ -\sin(\theta) & 0 & \cos(\theta) \end{pmatrix} \quad (2)$$

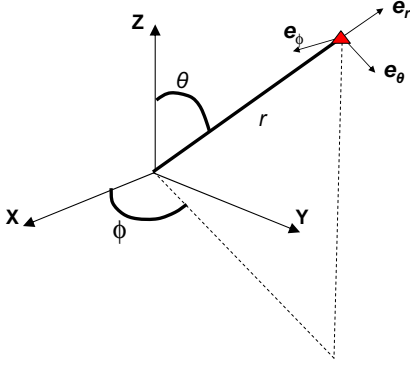


Fig. 5. Spherical and local coordinate systems

Applying Newton's laws of motion in the local coordinate system, the following equations are obtained:

$$\begin{aligned} r\ddot{\theta} - r \sin(\theta) \cos(\theta) \dot{\phi}^2 + 2\dot{\theta}\dot{r} &= \frac{F_\theta}{m} \\ r \sin(\theta) \ddot{\phi} + 2r \cos(\theta) \dot{\phi}\dot{\theta} + 2 \sin(\theta) \dot{\phi}\dot{r} &= \frac{F_\phi}{m} \\ \ddot{r} - r\dot{\theta}^2 - r \sin^2(\theta) \dot{\phi}^2 &= \frac{F_r}{m} \end{aligned} \quad (3)$$

where m is the kite mass. The external forces F_θ , F_ϕ and F_r include the contributions of gravitational force mg , aerodynamic force \vec{F}^{aer} and force F^c exerted by the kite on the lines. Their relations, expressed in the local coordinates, are given by:

$$\begin{aligned} F_\theta &= \sin(\theta)mg + F_\theta^{\text{aer}} \\ F_\phi &= F_\phi^{\text{aer}} \\ F_r &= -\cos(\theta)mg + F_r^{\text{aer}} - F^c \end{aligned} \quad (4)$$

where forces are assumed positive in the direction of basis vectors e_θ , e_ϕ and e_r .

\vec{F}^{aer} depends on the effective wind speed \vec{W}_e , which in the local system is computed as:

$$\vec{W}_e = \vec{W}_a - \vec{W}_l \quad (5)$$

\vec{W}_a is the kite speed, expressed in the local system as:

$$\vec{W}_a = \begin{pmatrix} \dot{\theta}r \\ \dot{\phi}r \sin \theta \\ \dot{r} \end{pmatrix} \quad (6)$$

Let us consider now the kite wind coordinate system, with the origin in the kite center of gravity, \vec{x}_w basis vector aligned with the effective wind speed vector, \vec{z}_w basis vector contained by the kite longitudinal mirror symmetry plane and pointing from the top surface of the kite to the bottom, and wind \vec{y}_w basis vector completing the right handed system.

In the wind coordinate system the aerodynamic force \vec{F}_w^{aer} is given by:

$$\vec{F}_w^{\text{aer}} = F_D \vec{x}_w + F_L \vec{z}_w \quad (7)$$

where F_D is the drag force and F_L is the lift force, computed as:

$$\begin{aligned} F_D &= -\frac{1}{2} C_D A \rho |W_e|^2 \\ F_L &= -\frac{1}{2} C_L A \rho |W_e|^2 \end{aligned} \quad (8)$$

where ρ is the air density, A is the kite characteristic area, C_L and C_D are the kite lift and drag coefficients. All of these variables are supposed to be constant. \vec{F}^{aer} can then be expressed in the local coordinate system as a nonlinear function of several arguments:

$$\vec{F}^{\text{aer}} = \begin{pmatrix} F_\theta^{\text{aer}}(\theta, \phi, r, \psi, \vec{W}_e) \\ F_\phi^{\text{aer}}(\theta, \phi, r, \psi, \vec{W}_e) \\ F_r^{\text{aer}}(\theta, \phi, r, \psi, \vec{W}_e) \end{pmatrix} \quad (9)$$

Angle ψ indicated in (9) is the control variable, defined by

$$\psi = \arcsin\left(\frac{\Delta l}{d}\right) \quad (10)$$

with d being the distance between the two lines fixing points at the kite and Δl the length difference of the two lines. Angle ψ influences the kite motion by changing the direction of the vector \vec{F}^{aer} .

As the kite can exert on the lines positive forces only, force F^c is such that $F^c \geq 0$. Moreover, it is considered that F^c is measured and that, using a local controller of the drives, it is regulated in such a way that $\dot{r}(t) \approx \dot{r}_{\text{ref}}(t)$ where $\dot{r}_{\text{ref}}(t)$ is suitably chosen. It results that $F^c(t) = F^c(\theta, \phi, r, \theta, \dot{\phi}, \dot{r}, \dot{r}_{\text{ref}}, \vec{W}_e)$. Since the power is $P = \dot{r}F^c$, in the traction phase $\dot{r}_{\text{ref}}(t) > 0$ is chosen and a positive power is generated, the kite getting farther from the origin and the drives acting as generators. In the recovery phase, $\dot{r}_{\text{ref}}(t) < 0$ is required, since the lines length has to be reduced: a negative power results, to be provided by the drives acting as motors.

Thus the system dynamics are of the form:

$$\dot{x}(t) = g(x(t), u(t), W_x(t), \dot{r}_{\text{ref}}(t), \vec{W}_t(t)) \quad (11)$$

where $x(t) = [\theta(t) \ \phi(t) \ r(t) \ \dot{\theta}(t) \ \dot{\phi}(t) \ \dot{r}(t)]^T$ and $u(t) = \psi(t)$. All the model states are supposed to be measured, to be used for feedback control.

III. KITE CONTROL USING MPC

Control problem and related objectives are now described. As highlighted in the Introduction, the main objective is to generate energy by a suitable control action on the kite. In order to accomplish this aim, a two-phase cycle has been defined. The two phases are referred to as the *traction phase* and the *recovery phase*. For the whole cycle to be generative, the total amount of energy produced in the first phase has to be greater than the energy spent in the second one to recover the kite before starting another cycle. In both phases, MPC controllers are designed, according to their own functional, state and input constraints and terminal conditions.

The control move computation is performed at discrete time instants defined on the basis of a suitably chosen sampling period Δ_t . At each sampling time $t_k = k\Delta_t$, $k \in \mathbb{Z}^+$, the measured values of the state $x(t_k)$ and of the wind speed $W_x(t_k)$, together with the chosen value of the reference speed $\dot{r}_{\text{ref}}(t_k)$, are used to compute the control move through the optimization of a performance index of the form:

$$J(U, t_k, T_p) = \int_{t_k}^{t_k+T_p} L(\tilde{x}(\tau), \tilde{u}(\tau), W_x(\tau), \dot{r}_{\text{ref}}(\tau)) d\tau \quad (12)$$

where $T_p = N_p \Delta_t$, $N_p \in \mathbb{Z}^+$ is the prediction horizon, $\tilde{x}(\tau)$ is the state predicted inside the prediction horizon according to the state equation (11), using $\vec{W}_t(t) = 0$, $\tilde{x}(t_k) = x(t_k)$ and the piecewise constant control input $\tilde{u}(t)$ belonging to the sequence $U = \{\tilde{u}(t)\}$, $t \in [t_k, t_k+T_p]$ defined as:

$$\tilde{u}(t) = \begin{cases} \bar{u}_i, \forall t \in [t_i, t_{i+1}], i = k, \dots, k + T_c - 1 \\ \bar{u}_{k+T_c-1}, \forall t \in [t_i, t_{i+1}], i = k + T_c, \dots, k + T_p - 1 \end{cases} \quad (13)$$

where $T_c = N_c \Delta_t$, $N_c \in \mathbb{Z}^+$, $N_c \leq N_p$ is the control horizon.

As it will be discussed later, the function $L(\cdot)$ in (12) is suitably defined on the basis of the performances to be achieved in the operating phase the kite lies in. Moreover, in order to take into account physical limitations on both the kite behaviour and the control input ψ in the different phases, linear constraints of the form $F\tilde{x}(t) + G\tilde{u}(t) \leq H$ have been included too.

Thus the predictive control law is computed using a receding horizon strategy:

- 1) At time instant t_k , get $x(t_k)$.
- 2) Solve the optimization problem:

$$\min_U J(U, t_k, T_p) \quad (14a)$$

subject to

$$\dot{\tilde{x}}(t) = g(\tilde{x}(t), \tilde{u}(t), W_x(t), \dot{r}_{\text{ref}}(t)) \quad (14b)$$

$$F\tilde{x}(t) + G\tilde{u}(t) \leq H, \forall t \in [t_k, t_k+T_p] \quad (14c)$$

- 3) Apply the first element of the solution sequence U to the optimization problem as the actual control action $u(t_k) = \tilde{u}(t_k)$.
- 4) Repeat the whole procedure at the next sampling time t_{k+1} .

Therefore the predictive controller results to be a nonlinear static function of the system state x , the nominal measured wind speed W_x and the reference \dot{r}_{ref} :

$$\psi(t_k) = f(x(t_k), W_x(t_k), \dot{r}_{\text{ref}}(t_k)) \quad (15)$$

A. Traction phase

The aim of this phase is to obtain as much mechanical energy as possible from the wind stream. The following initial state value ranges are considered to start the *traction phase*:

$$\begin{aligned} \underline{\theta}_I &\leq \theta(t) \leq \bar{\theta}_I \\ |\phi(t)| &\leq \bar{\phi}_I \\ \underline{r}_I &\leq r(t) \leq \bar{r}_I \end{aligned} \quad (16)$$

with

$$\begin{aligned} 0 &< \underline{\theta}_I < \bar{\theta}_I < \pi/2 \\ 0 &< \bar{\phi}_I < \pi/2 \end{aligned} \quad (17)$$

Roughly speaking, the *traction phase* begins when the kite is flying in a symmetric zone with respect to the X axis, at an altitude Z_I such that $(\underline{r}_I \cos \bar{\theta}_I \leq Z_I \leq \bar{r}_I \cos \underline{\theta}_I)$. When the *traction phase* starts, a positive value \bar{r} of \dot{r}_{ref} is set so that the kite flies with increasing values of r while applying a traction force F^c on the lines, thus generating mechanical power. The value \bar{r} is chosen to get a good compromise between obtaining high traction force actions and high line winding speed values. Basically, the stronger the wind, the higher the values of \bar{r} that can be set obtaining high force values. Control system objective adopted in the *traction phase* is to maximize the energy generated in the interval $[t_k, t_k + T_p]$, while satisfying constraints concerning state and input values. Mechanical power generated at each instant is $P = \dot{r}F^c$, thus the following cost function is chosen to be minimized in MPC design (14):

$$J(t_k) = - \int_{t_k}^{t_k+T_p} (\dot{r}(\tau)F^c(\tau)) d\tau \quad (18)$$

During the whole phase the following state constraint is considered to keep the kite sufficiently far from the ground:

$$\theta(t) \leq \bar{\theta} \quad (19)$$

with $\bar{\theta} < \pi/2$. Actuator physical limitations give rise to the constraints:

$$\begin{aligned} |\psi(t)| &\leq \bar{\psi} \\ |\dot{\psi}(t)| &\leq \bar{\dot{\psi}} \end{aligned} \quad (20)$$

To complete the *traction phase* description, ending conditions have to be introduced. Each kite line is initially wrapped around a pulley and unrolls while the kite gets farther. When r reaches a value \bar{r} it is necessary to wrap the lines back, in order to make the KiteGen prototype able to start a new cycle. Therefore, when the following condition is reached the *traction phase* ends and the *recovery phase* can start:

$$r(t) = \bar{r} \quad (21)$$

B. Recovery phase

During this phase the kite lines must be wrapped back using the least amount of energy, in order to maximize the net energy gain of the whole cycle. The *recovery phase* has been divided into three sub-phases.

In the first sub-phase, $\dot{r}_{\text{ref}}(t)$ is chosen to smoothly decrease towards zero from value \bar{r} . The control objective is to move the kite in a zone with low values of θ and high values of $|\phi|$, where effective wind speed \vec{W}_e and force F^c are low and the kite is ready to be recovered with low energy expense. Positive values $\bar{\theta}_{II}$ and $\underline{\phi}_{II}$ of θ and ϕ respectively are introduced to identify this zone. The following cost function is considered:

$$J(t_k) = \int_{t_k}^{t_k+T_p} \theta^2(\tau) (|\phi(\tau)| - \pi/2)^2 d\tau \quad (22)$$

Once the following condition is reached:

$$\begin{aligned} |\phi(t)| &\geq \underline{\phi}_{II} \\ \theta(t) &\leq \bar{\theta}_{II} \end{aligned} \quad (23)$$

the first recovery part ends.

When the second recovery sub-phase begins, $\dot{r}_{\text{ref}}(t)$ is chosen to smoothly decrease from zero to a negative constant value $\underline{\dot{r}}$. Such a value is chosen to give a good compromise between high winding back speed and low F^c values.

During this second recovery sub-phase, control objective is to minimize the energy spent to wind back the lines, thus the following cost function is considered:

$$J(t_k) = \int_{t_k}^{t_k+T_p} |\dot{r}(\tau)| F^c(\tau) d\tau \quad (24)$$

The second sub-phase ends when the following condition is satisfied:

$$r_I \leq r(t) \leq \bar{r}_I \quad (25)$$

which means when r is among the possible *traction phase* initial state values. Then, the third recovery sub-phase begins and $\dot{r}_{\text{ref}}(t)$ is chosen to smoothly increase towards zero from the negative value $\underline{\dot{r}}$. Control objective is to move the kite in the *traction phase* starting zone, expressed by (16). Cost function $J(t_k)$ is set as follows:

$$J(t_k) = \int_{t_k}^{t_k+T_p} (|\theta(\tau) - \theta_1| + |\phi(\tau)|) d\tau \quad (26)$$

where $\theta_1 = (\underline{\theta}_I + \bar{\theta}_I)/2$. Ending conditions for the whole *recovery phase* coincide with starting conditions for the *traction phase*.

During the whole *recovery phase* the state constraint expressed by (19) and the input constraints (20) are considered in the control optimization problems.

IV. "FAST" MPC IMPLEMENTATION

For any of the MPC controller previously described, control $\psi(t_k)$ results to be the nonlinear static function given by (15), which can be rewritten as:

$$\psi(t_k) = f(w(t_k))$$

Where $w(t_k) = (x(t_k), W_x(t_k), \dot{r}_{\text{ref}}(t_k))^T$. For a given $w(t_k)$, the value of the function $f(w(t_k))$ is typically computed by solving at each sampling time t_k the constrained optimization problem (14). However, an online solution of the optimization problem at each sampling time cannot be performed at the sampling period required for this application, of the order of 0.1 s. For example, the average computation time of MPC implementation proposed in [4], for the flight control of the same kite model in a simpler situation (periodic orbit with constant r), resulted to be about 0.45 s on a workstation. An approach to overcome this problem is to evaluate off line a certain number of values of $f(w)$ to be used to find an approximation \hat{f} of f , suitable to be used for online implementation.

To be more specific, consider a bounded region $W \subset \mathbb{R}^8$ where w can evolve.

A number ν of values of $f(w)$ may be derived by performing offline the MPC procedure starting from a set of values $W_\nu = \{\tilde{w}_k \in W, k = 1, \dots, \nu\}$, so that:

$$\tilde{\psi}_k = f(\tilde{w}_k), \quad k = 1, \dots, \nu \quad (27)$$

The aim is to derive, from these known values of $\tilde{\psi}_k$ and \tilde{w}_k and from known properties of f , an approximation \hat{f} of f and a measure of the approximation error. Neural networks have been used in [7] and [8] for such approximation. The problems with neural networks are the trapping in local minima during the learning phase and the difficulty of handling the constraints in the image set of the function to be approximated. Moreover, no measure of the approximation error is provided. In order to overcome these drawbacks, a Set Membership approach has been proposed in [5] for an MPC formulation involving linear models. Basic to this approach is the observation that in order to derive a measure of the approximation error achieved by any method, the knowledge of $f(\tilde{w}_k)$, $k = 1, \dots, \nu$ is not sufficient, but some additional information on f is needed. In this paper it is assumed that $f \in \mathcal{F}_\gamma$, where \mathcal{F}_γ is the set of all Lipschitz functions on W , with Lipschitz constant γ . Note that stronger assumptions cannot be made, since even in the simple case of linear dynamics and quadratic functional, f is a piecewise linear continuous function [9], [10]. An additional information to be used in the approximation is the input saturation condition giving $|f(w)| \leq \bar{\psi}$. These information on function f , combined with the knowledge of the value of the function at the points $\tilde{w}_k \in W$, $k = 1, \dots, \nu$, allows to conclude that $f \in FFS$, where the set FFS (Feasible Functions Set), defined as:

$$FFS = \{f \in \mathcal{F}_\gamma : |f(w)| \leq \bar{\psi}; f(\tilde{w}_k) = \tilde{\psi}_k, k = 1, \dots, \nu\} \quad (28)$$

summarizes the overall information on f . Making use of such overall information, Set Membership theory allows to derive an optimal estimate of f and its approximation error, in term of the $L_p(W)$ norm $p \in [1, \infty]$, defined as $\|f\|_p \doteq [\int_W |f(w)|^p dw]^{\frac{1}{p}}$, $p \in [1, \infty)$ and $\|f\|_\infty \doteq \text{ess-sup}_{w \in W} |f(w)|$. For given $\hat{f} \approx f$, the related L_p approximation error is $\|f - \hat{f}\|_p$. This error cannot be exactly computed, but its tightest bound is given by:

$$\|f - \hat{f}\|_p \leq \sup_{\tilde{f} \in FFS^T} \|\tilde{f} - \hat{f}\|_p \doteq E(\hat{f}) \quad (29)$$

where $E(\hat{f})$ is called (guaranteed) *approximation error*.

A function f^* is called an *optimal approximation* if:

$$E(f^*) = \inf_{\hat{f}} E(\hat{f}) \doteq r_p$$

The quantity r_p , called *radius of information*, gives the minimal L_p approximation error that can be guaranteed.

Let us define:

$$\begin{aligned} \bar{f}(w) &\doteq \min \left[\bar{\psi}, \min_{k=1, \dots, \nu} (\tilde{\psi}_k + \gamma \|w - \tilde{w}_k\|) \right] \\ \underline{f}(w) &\doteq \max \left[-\bar{\psi}, \max_{k=1, \dots, \nu} (\tilde{\psi}_k - \gamma \|w - \tilde{w}_k\|) \right] \end{aligned} \quad (30)$$

It results that the function:

$$f^*(w) = \frac{1}{2}[\bar{f}(w) + \underline{f}(w)] \quad (31)$$

is an optimal approximation for any $L_p(W)$ norm, with $p \in [1, \infty]$ [6].

Moreover, the approximation error of f^* is pointwise bounded as:

$$|f(w) - f^*(w)| \leq \frac{1}{2}|\bar{f}(w) - \underline{f}(w)|, \forall w \in W$$

and is pointwise convergent to zero:

$$\lim_{\nu \rightarrow \infty} |f(w) - f^*(w)| = 0, \forall w \in W \quad (32)$$

Thus, evaluating $\sup_{w \in W} |\bar{f}(w) - \underline{f}(w)|$, it is possible to decide if the chosen ν is sufficient to achieve a desired accuracy in the estimation of f or if ν has to be increased. An estimate $\hat{\gamma}$ of γ can be derived as follows:

$$\hat{\gamma} = \inf_{\gamma: \bar{f}(\bar{w}_k) \geq \psi_k, k=1, \dots, \nu} \gamma \quad (33)$$

Such estimate is convergent to γ :

$$\lim_{\nu \rightarrow \infty} \hat{\gamma} = \gamma \quad (34)$$

Note that convergence results (32) and (34) hold if $\lim_{\nu \rightarrow \infty} d(W_\nu, W) = 0$, where $d(W_\nu, W)$ is the Hausdorff distance between sets W_ν and W . Such a condition is satisfied if, for example, W_ν is obtained by uniform gridding of W .

Thus, the MPC control can be approximately implemented online, by simply evaluating the function $f^*(w_{t_k})$ at each sampling time:

$$\psi_{t_k} = f^*(w_{t_k})$$

Increasing ν the approximation error decreases at the cost of increased computing time. In the numerical case reported below, using $\nu = 10000$ the error in computing ψ_t is less than 1% in all operating conditions. The corresponding mean time required for the computation of control move $f^*(w_{t_k})$ implemented on dSpace[®] MicroAutobox (800 MHz clock) is about 0.01 s, largely lower than the required sampling time.

V. SIMULATION RESULTS

The results of three simulations are presented here. The values of model and control parameters are reported in Table I. Table II contains the state values which identify each phase starting and ending conditions and the values of state and input constraints.

Note that since the lines unroll at a speed of 0.5 m/s for about 180 m, the *traction phase* lasts about 360 s. In the *recovery phase* the lines wrapping back speed is -2.3 m/s, thus the second recovery sub-phase lasts about 80 s. The nominal wind speed is given as (1):

$$W_x(Z) = \begin{cases} 0.02Z + 4 & \text{if } Z \leq 100m \\ 0.0086(Z - 100) + 6 & \text{if } Z > 100m \end{cases} \text{ m/s} \quad (35)$$

TABLE I
MODEL AND CONTROL PARAMETERS

m	2.5	kite mass (kg)
A	5	characteristic area (m ²)
ρ	1.2	air density (kg/m ³)
CL	1.2	lift coefficient
CD	0.15	drag coefficient
\bar{r}	0.5	<i>traction phase</i> reference \dot{r}_{ref} (m/s)
\underline{r}	-2.3	<i>recovery phase</i> reference \dot{r}_{ref} (m/s)
T_c	0.1	sample time (s)
N_c	1	control horizon
N_p	25	prediction horizon

TABLE II
STATE AND INPUT CONSTRAINTS, CYCLE STARTING AND ENDING CONDITIONS

θ_I	35°	<i>Traction phase</i> starting conditions
θ_I	45°	
ϕ_I	5°	
r_I	95 m	
\bar{r}_I	105 m	
\bar{r}	280 m	<i>Traction phase</i> ending condition
ϕ_{II}	30°	2 nd <i>Recovery</i> sub-phase starting conditions
θ_{II}	60°	
θ	85°	State constraint
$\bar{\psi}$	4°	Input constraints
$\dot{\psi}$	20 °/s	

Nominal wind speed is 4 m/s at 0 m of altitude and grows linearly to 6 m/s at 100 m and up to 7.7 m/s at 300 m of height. In the first simulation, no wind turbulence was considered, so $W_t(t) = 0$. In the second simulation a lateral sinusoidal wind turbulence $W_{t,y}(t)$ along Y axis was introduced:

$$W_{t,y}(t) = 3 \sin(\omega_0 t) \text{ m/s} \quad (36)$$

with $\omega_0 = 2\pi/10$ rad/s. Finally, in the third simulation the following vertical wind turbulence $W_{t,z}(t)$ along Z axis was introduced:

$$W_{t,z}(t) = \begin{cases} 0 & \text{if } t \leq 100s \\ -1.5 & \text{if } 100 < t \leq 200s \\ 0 & \text{if } 200 < t \leq 350s \\ -1.5 & \text{if } t > 350s \end{cases} \text{ m/s} \quad (37)$$

The disturbance described by (37) includes two vertical wind steps: the first lasts 100 s during the *traction phase*, the second is applied over the whole *recovery phase*. Note that the $W_{t,y}$ and $W_{t,z}$ amplitudes are equal to 50% and 25% of nominal wind speed at 100 meters of altitude, thus introducing quite strong perturbations into the system.

Fig. 6 shows the trajectory of the kite in nominal conditions. Fig. 7 depicts some orbits traced by the kite during the *traction phase*: it can be seen that the kite follows “lying eight” orbits in this phase, with a period of about 5 s; about 75 orbits are thus completed in a single *traction phase*. Power generated during the cycle is reported in Fig. 8: the mean value is 1.58 kW, which corresponds to 733 kJ per cycle. Fig. 9 and 10 show the trajectory of the kite and the power generated in presence of lateral wind disturbances described

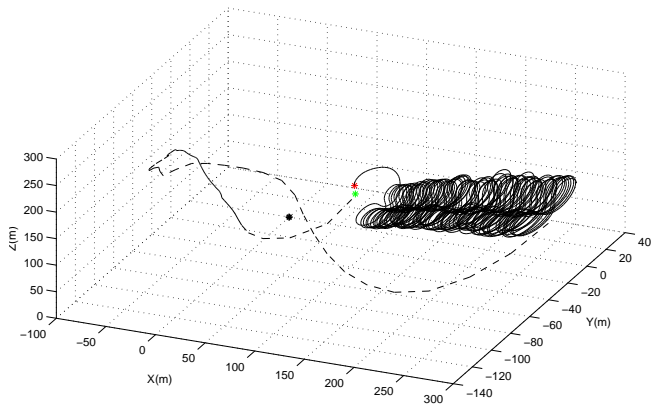


Fig. 6. Kite trajectory with nominal conditions: *traction phase*(solid) and *recovery phase*(dashed)

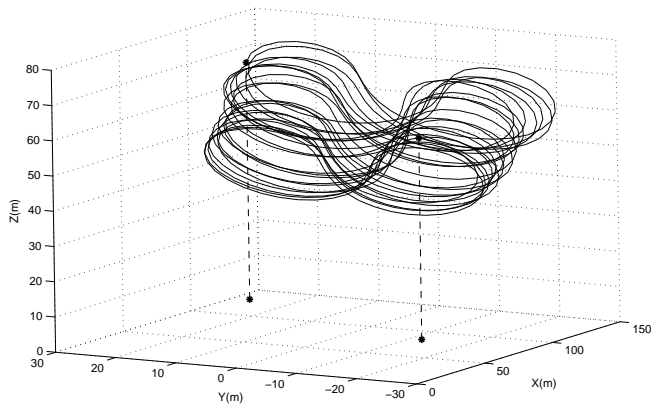


Fig. 7. Some *traction phase* orbits

by (36): the cycle is completed and the generated energy value, 727 kJ, is almost the same that was obtained without disturbances, showing the good tolerance of the control system to lateral wind turbulence.

Simulation results in presence of vertical turbulence described by (37) are reported in Fig. 11 and 12: the first wind step leads to a lower value of generated energy (681 kJ) but the cycle was completed anyway, showing good system robustness also in presence of severe vertical wind disturbances.

VI. CONCLUSIONS AND FUTURE DEVELOPMENTS

The paper has presented a first study aimed to investigate the capability of controlling tethered airfoils in order to devise a new class of wind generators able to overcome the main limitations of the present aeolian technology based on wind mills.

The obtained results appear to be very encouraging, but are based on simulations carried on a kite model taken from the literature, which certainly can give only approximate description of involved dynamics. Indeed, accurate modeling the dynamic of non rigid airfoils is well known to be a quite challenging task and it can be expected that the control design based on this model may not perform in a satisfactory

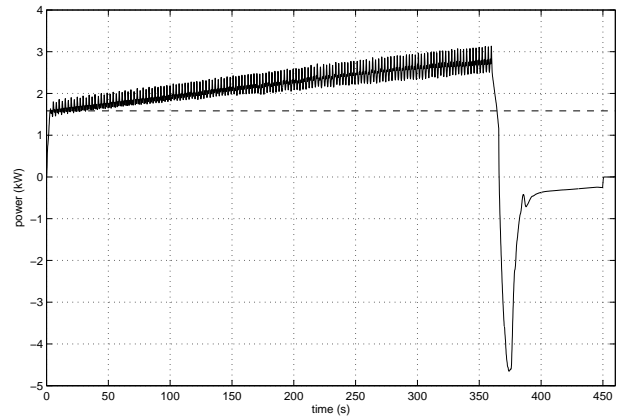


Fig. 8. Instant (solid) and mean (dashed) power generated in a single cycle, nominal conditions

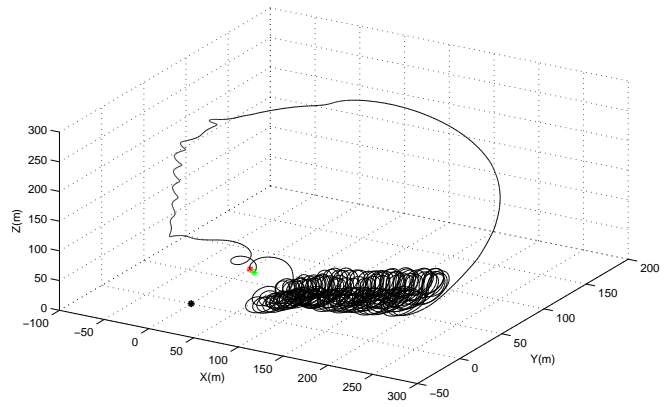


Fig. 9. Kite trajectory with lateral wind turbulence

way on the prototype under construction. Thus, advanced methods for the identification of complex nonlinear systems such as [11], [12] are planned to be applied to measurements obtained from the prototype under construction, in order to derive more accurate models, sufficient to obtain good performances from the NMPC design.

It must be remarked that the results reported in the present paper are related to the small kite (5 m^2 characteristic area) planned for the prototype under construction. With a kite area of 50 m^2 , simulations give about 200 kW power generated with 12 m/s wind speed. A wind turbine of the same power is 40 m high, weights about 62 t and costs about 900.000,00 euros. The expected KiteGen weight and cost are about 8 t and 60.000,00 euros respectively. These values, even if only partially confirmed by experiments, demonstrate the potentialities of using controlled airfoils for the generation of electric energy. Indeed, even greater potentialities are offered by the more efficient configuration that will be investigated at Respira Lab in case of success of the first prototype. In this configuration, the airfoils are connected to a vertical axis rotative turbine (see Fig. 13), and the control is designed to maximize the power transmitted by the airfoils to the turbine arms, suitably connected to the electric generators. According to our preliminary evaluations, it is expected that

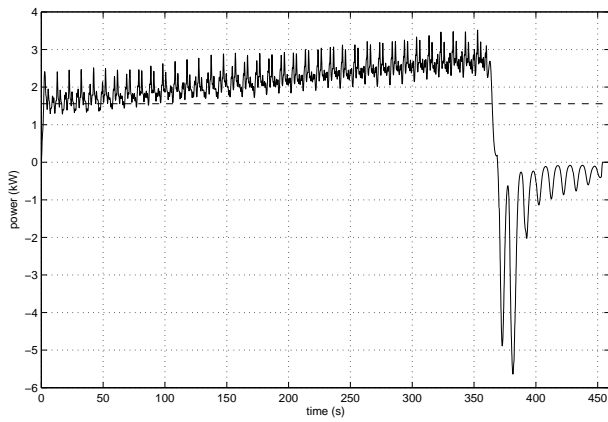


Fig. 10. Instant (solid) and mean (dashed) power generated in a single cycle, lateral wind turbulence

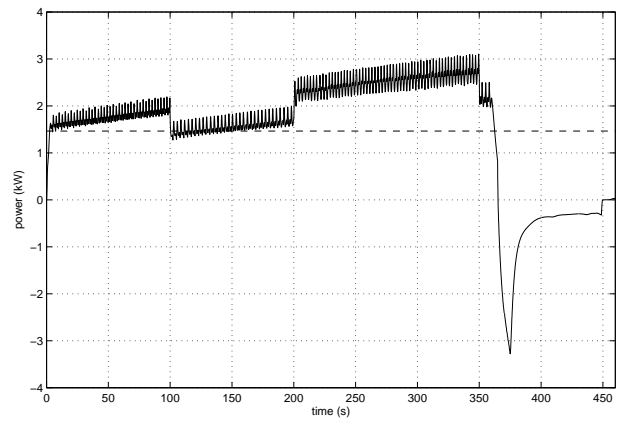


Fig. 12. Instant (solid) and mean (dashed) power generated in a single cycle, vertical wind turbulence

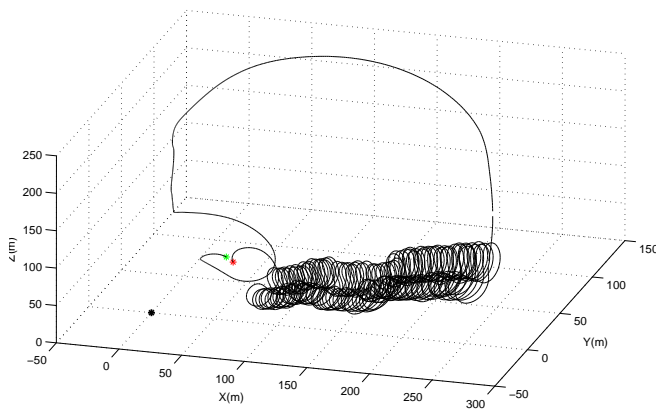


Fig. 11. Kite trajectory with vertical wind turbulence

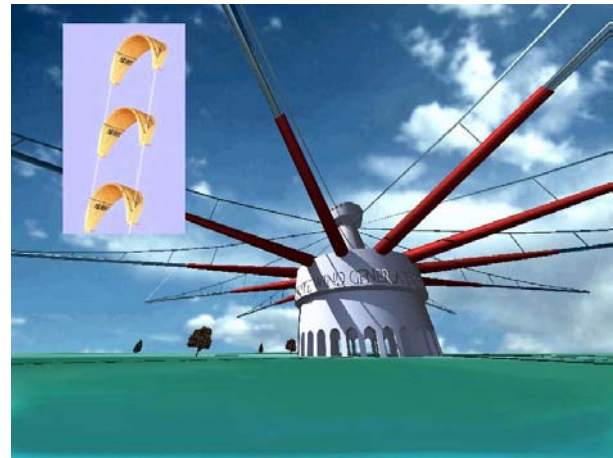


Fig. 13. A more powerful and effective configuration of KiteGen

wind generators of this type may have much lower electric energy production costs than actual wind farms (by a factor up to 10-20) and could generate up to 250 MW/km^2 , vs. 3 MW/km^2 of wind farms.

REFERENCES

- [1] Worldwatch Institute, "Renewables 2005: Global Status Report" prepared for the Renewable Energy Policy Network, Washington DC, 2005. <http://www.REN21.net>
- [2] "Smart control system exploiting the characteristics of generic kites or airfoils to convert energy", *European patent # 02840646*, inventor: M. Ippolito, December 2004
- [3] *Vestas Wind Systems A/S website*: <http://www.vestas.com>
- [4] M. Diehl, "Real-Time Optimization for Large Scale Nonlinear Processes", PhD thesis, University of Heidelberg, Germany, 2001.
- [5] M. Canale and M. Milanese, "A fast implementation of model predictive control techniques", in *16th IFAC World Congress*, Prague, Czech Republic, July 2005.
- [6] M. Canale, L. Fagiano, M. Milanese, "Fast implementation of nonlinear model predictive controllers". Technical Report CaFM-1-2006. Dipartimento di Automatica e Informatica, Politecnico di Torino, 2006.
- [7] T. Parisini and R. Zoppoli, "A receding-horizon regulator for nonlinear systems and a neural approximation". *Automatica* **31**(10), 1443–1451, 1995.
- [8] D. R. Ramirez, M. R. Arahal and E. F. Camacho "Min-max predictive control of a heat exchanger using a neural network solver" *IEEE Transactions on Control Systems Technology* **12**(5), 776–786, 2004.
- [9] M.M. Seron, G.C. Goodwin and J.A. De Doná, "Characterization of receding horizon control for constrained linear systems", *Asian Journal of Control* **5**(2), 271–286, 2003.
- [10] A. Bemporad, M. Morari, V. Dua and E.N. Pistikopoulos "The explicit linear quadratic regulator for constrained systems", *Automatica* **38**, 3–20, 2002.
- [11] M. Milanese and C. Novara, "Set membership identification of nonlinear systems", *Automatica*, vol. 40, pp. 957–975, 2004.
- [12] M. Milanese, C. Novara and L. Pivano, "Structured Experimental Modelling of Complex Nonlinear Systems", *42nd IEEE Conference on Decision and Control*, Maui, Hawaii, 2003.